

Roughening of a propagating planar crack front

J. A. Åström,¹ M. J. Alava,² and J. Timonen¹

¹*Department of Physics, University of Jyväskylä, P.O. Box 35, FIN-40351 Jyväskylä, Finland*

²*Laboratory of Physics, Helsinki University of Technology, P.O. Box 1100, FIN-02015 TKK, Finland*

(Received 14 February 2000)

A numerical model of the front of a planar crack propagating between two connected elastic plates is investigated. The plates are modeled as square lattices of elastic beams. The plates are connected by similar but breakable beams with a randomly varying stiffness. The crack is driven by pulling both plates at one end in Mode I at a constant rate. We find $\zeta=1/3$, $z=4/3$, and $\beta=1/4$ for the roughness, dynamical, and growth exponents, respectively, that describe the front behavior. This is similar to continuum limit analyses based on a perturbative stress-intensity treatment of the front [H. Gao and J. R. Rice, *J. Appl. Mech.* **56**, 828 (1989)]. We discuss the differences to recent experiments.

PACS number(s): 62.20.Mk, 46.50.+a, 68.35.Ct

It was pointed out by Mandelbrot *et al.* [1] that the roughness of cracks may be related to the fracture toughness of the material (i.e., the energy needed to create a crack) if measured in the out-of-plane direction. The in-plane roughness of a growing planar crack front is not similar in this respect but relates to the strength of the material. The front has to pass regions of varying local strength, perhaps in the sense of the Griffith surface energy, or, more generally, local elastic energy barriers must be overcome by the crack for it to propagate. The physics of the propagation becomes dependent on the details of the crack-front elasticity.

Suppose that the total length of a planar crack front is L , and that there are $N=L/\delta L$ local elastic barriers (c.f. Fig. 1). Assume that the stiffnesses of these are $E_i, i=1, \dots, N$, and that each of them breaks at a critical strain ϵ_c . If the strain is uniformly distributed, a total external force $N\langle E_i \rangle \epsilon_c$ will be needed to initiate the propagation of a straight, zero-roughness crack. If, on the other hand, it is the stress which is shared globally along the crack front, the crack will first begin to propagate at the location of the minimum local stiffness E_{\min} . This happens when the external force is $NE_{\min}\epsilon_c$, which for a broad distribution of E_i is considerably lower than $N\langle E_i \rangle \epsilon_c$. For uncorrelated, random E_i , the initial phase of the crack growth would now be related to the unrelated burst events along the crack front. This would lead to a slightly rough crack front with a random deposition-like scaling in contrast with the previous case. This thought experiment demonstrates that it is the stress-transfer relation which is crucial for the shape of the crack front.

The scaling of the roughness of crack fronts is still a controversial issue since the theoretical suggestions for the roughness and dynamic exponents reported in the literature show little agreement with experiments. In a recent experiment on weakly coupled blocks [2] $\zeta=0.63\pm 0.03$ was found on length scales up to a few millimeters. The theoretical predictions have usually been based on one-dimensional models of cracks moving in a heterogeneous potential [3,4]. Gao and Rice [5] presented a continuum elasticity calculation in first order perturbation theory of the stress-intensity factor along a crack front that deviates slightly from a straight line. The stress intensity factor $f(x)$ was expressed in the form

$$f(x) = -k \int \frac{u(x) - u(x_1)}{|x - x_1|^2} dx_1, \quad (1)$$

where x is the space coordinate along the front, and $u(x)$ is the location of the front. The kinetic roughening of a crack front governed by Eq. (1) has been studied thoroughly [6–8]. The values of the roughness, dynamic and growth exponents were in Ref. [8] found to be $\zeta=1/3$, $z=4/3$, and $\beta=1/4$, respectively. This agrees well with the earlier functional renormalization group result by Ertaş and Kardar [9]. Thus there is a controversial situation in that real crack fronts seem to be much rougher than what the theoretical estimates for ζ imply.

In this paper we consider the crack roughening in a beam lattice model driven slowly, in a setup that roughly corresponds to the constant-velocity ensemble in depinning models, and which is similar to the experimental setup in [2]. Beam lattices form a straightforward discretization of an elastic solid, and we should thus have a theoretical model which contains no major approximations when compared to the experimental system. The model should hence be useful when discussing the discrepancy between theory and experiment. We use here a cubic lattice geometry, with the beams as the bonds connecting the lattice sites. The beams have zero mass, unlike the sites. They are assumed to have a square cross section, and we use the stiffness matrix of a slender beam (i.e., bending dominates over shear deforma-

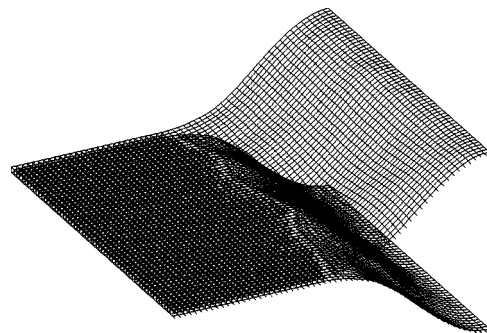


FIG. 1. A crack front propagating in a lattice of size $60 \times 60 \times 1$.

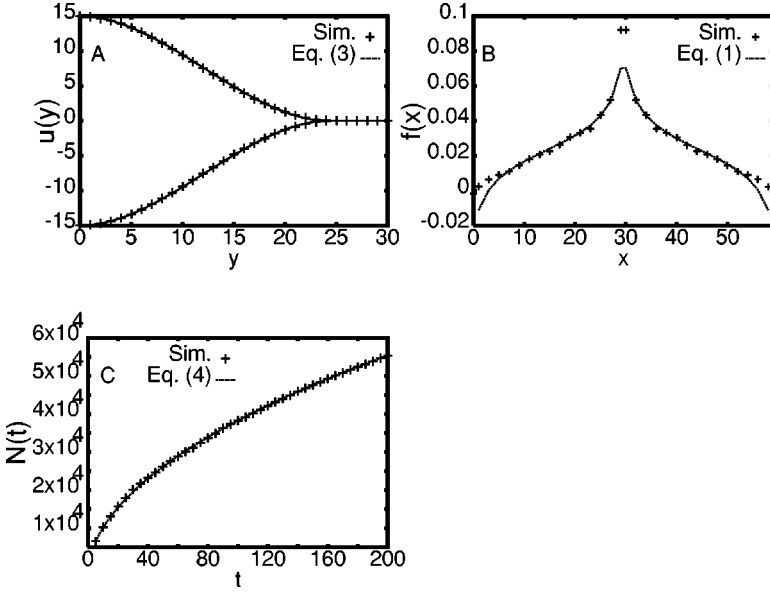


FIG. 2. (A) Equation (3) compared with simulation results. (B) The simulated stress-intensity distribution ($f(x)$) in a 'V' shaped crack front, compared with the stress-intensity distribution given by Eq. (1) for the same front shape. (C) Equation (4) compared with the simulations.

tions), which can be derived from the linear theory of elasticity [10]. Notice that we only use linear elasticity, and therefore neglect higher order terms in the displacements of the sites brought about by deformations. In other words, our model is strictly correct only if the beams break already at an infinitesimal deformation. The length of the beams is set to unity, their Poisson ratio is assumed to be zero, and the cross-sectional area is set to $w^2 = (0.7)^2$. The parameters are chosen based on numerical efficiency. In the model the force needed to elongate a beam a unit distance is $E_i w^2$, and to shear a beam, $E_i w^4$. The torque needed to bring about a unit torsional rotation and a unit off-axis rotation of one of the ends of a beam are $E_i w^4/12$ and $E_i w^4/3$, respectively. The masses, the moments of inertia of the sites and the Young's moduli (E_i) of the beams are all random variables. The values are taken from the distribution a^{δ_i} , where $a=25$ is a constant and δ_i is an uncorrelated stochastic variable which takes values between 0 and 1. If a is close to unity there is little disorder in the system and the crack front will remain almost straight during its propagation. If a is very large (e.g., $a \sim 1000$), crack-front propagation is dominated by the disorder, and the roughness of the front will be essentially given by white noise. The largest lattices in the simulations are $L_x \times L_y \times L_z = 300 \times 400 \times 1$. The crack is confined to the xy plane, starting from $y=0$ at time $t=0$. Only the beams connecting the planes $z=0$ and $z=1$ are allowed to break. If these beams are stretched by more than $\epsilon_c = 1\%$, they break instantly and irreversibly. The two plates are separated by forcing the edge $z=0, y=0$ to move with velocity $v/2$ in the negative z direction, while the edge $z=1, y=0$ is forced to move with velocity $v/2$ in the positive z direction. This setup will induce a nonconstant average crack-front velocity as will be discussed later.

The dynamic displacements of the lattice sites are calculated using a discrete form of Newton's equations of motion including a small linear viscous dissipation term,

$$\left[\frac{M}{\Delta t^2} + \frac{C}{2\Delta t} \right] U(t + \Delta t) = \left[\frac{2M}{\Delta t^2} - K \right] U(t) - \left[\frac{M}{\Delta t^2} - \frac{C}{2\Delta t} \right] U(t - \Delta t), \quad (2)$$

where M is a diagonal mass matrix, K the stiffness matrix, C a diagonal damping matrix, U a vector containing the displacements from equilibrium of the lattice sites, Δt the length of the discrete time step, and t the time. In the simulations $C=I$, the unit matrix, and $M=440 \times I$. The stiffness matrix K is built from the stiffness matrices of the single beams (k_i) [11] by rotations defined by the beam orientations, and summing the elements that correspond to the same degree of freedom. An example of these systems is shown in Fig. 1. The size of this lattice is $60 \times 60 \times 1$, and the crack has propagated about halfway through the sample.

In order to investigate how well our lattice model describes a continuum elastic system we first compare the bending shape of the plates behind the crack tip. The continuum elastic equation for the equilibrium out-of-plane displacement u of a plate of linear size L in the xy plane is

$$\frac{Ew^3}{12(1-\sigma)} \nabla^4 u(x,y) = 0, \quad (3)$$

with the boundary conditions for clamped ends: $[\partial u(x,y)/\partial n] = 0$. Here n is the normal direction to the clamped end [12]. If there is no disorder, the crack front will be straight and therefore u will only be a function of y . If we furthermore apply the constraints $u(0) = 0$ and $u(L) = d$, we obtain the solution $u(y) = (3dy^2/L^2) - (2dy^3/L^3)$, which is compared with that of the numerical simulations in Fig. 2(A). The difference between the simulated and the continuum solution is practically nonexistent. To further check if Eq. (1) is consistent with the simulation model, we checked the correlation of the stress-intensity factor along the front during the simulations with that calculated from Eq. (1). This correlation was as such rather poor, but for very simple front shapes the agreement became better. A fairly good correspondence between the stress-intensity factors is demonstrated in Fig. 2(B), where one should note in particular the similarity of the long-range behavior of the effective kernels.

To further test the model we calculated by elasticity theory the expected propagation velocity of the crack. It can be shown that the shear stiffness of a plate scales as $1/L^3$, while the bending stiffness scales as $1/L^2$. This means that,

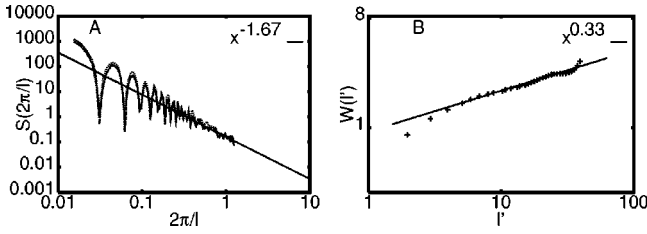


FIG. 3. The roughness exponent $\zeta=1/3$ of the perturbative solution compared with the simulation results. (A) The Fourier spectrum method, and (B) the variable bandwidth method.

when the crack has propagated for a sufficient distance, the out-of-plane bending moment at the crack tip will completely dominate over the tensile force. For this reason alone, a beam-lattice model is qualitatively different from, e.g., a fuse-lattice model [13]. Since the velocity v is given, we can estimate the time it takes for the crack to propagate from L to $L + \delta L$, which then gives the propagation velocity. We give the result as the total number (N) of broken beams as a function of time,

$$N(t) \propto L \left[\left(1 + \frac{t}{t_0} \right)^{1/2} - 1 \right], \quad (4)$$

where t_0 is a constant. Equation (4) is compared with simulation results in Fig. 2(C) ($a=25, L=60$). The difference between the simulation results and Eq. (4) is very small. We can thus conclude that the discrete lattice model used here is consistent with continuum elasticity theory. Consequently, the stress enhancement along the crack-front is expected to follow essentially the continuum behavior, which is necessary for the comparison of the respective roughening behaviors of the fronts.

We now turn to the simulation results for the kinetic roughness. We determine the roughness exponent ζ by the Fourier spectrum of the crack front, and by the variable bandwidth (local width) method [2]. For a self-affine profile the Fourier spectrum behaves as

$$S(2\pi/l) \equiv \left| \int u(x) e^{-i2\pi x/l} dx \right|^2 \propto (2\pi/l)^{1-2\zeta}. \quad (5)$$

For large wavelengths l , the Fourier spectrum will reflect the limited sample size due in particular to the periodic boundary conditions. For the spectral analysis we used a sample width of 400 lattice units. The simulation results for three different samples are shown in Fig. 3A. This is in decent agreement with the theoretical result $\zeta=1/3$. The self-affinity in the crack front develops relatively quickly for short wave lengths. Saturation of the roughness is only reached when the front has propagated a considerable distance from its initial position. This presents a numerical problem since the propagation velocity decreases according to Eq. (4). We therefore used a small transverse system size of only 40 lattice units, to allow the roughness to develop correlations over the whole front. We also removed the periodic boundary conditions. The average width of the front according to the variable bandwidth method should scale as $w(l') \propto (l')^\zeta$. The

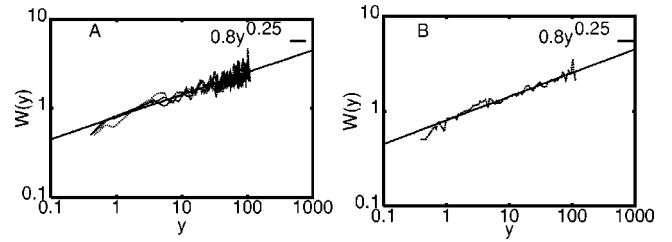


FIG. 4. The growth exponent $\beta=1/4$ of the perturbative solution compared with the simulation results. (A) The results for three separate samples and (B) the averaged growth.

simulation result averaged over several hundreds of samples is shown in Fig. 3(B). The roughness exponent is again consistent with the value $\zeta=1/3$.

The growth exponent β is defined by the initial increase of the roughness, or the average front width. This should scale with the average traveled distance of the front as $w(y) \propto y^\beta$. Recall that the average front velocity decreases with time, and thus one has to define β as a function of y [14]. The simulation results for three different, 400 lattice unit wide samples, are shown in Fig. 4(A). The average for the three samples is shown in Fig. 4(B). In both figures the roughness growth is compared with the perturbation theory result $\beta=1/4$, with very reasonable agreement.

Notice that the scaling exponents, as obtained above, indicate the value $z=4/3$ for the dynamical exponent via the scaling relation $z=\zeta/\beta$. An independent determination of z is rather tricky since, as explained above, saturation is numerically difficult to reach. On the other hand, z can be measured from the spreading of correlations in the front profile. As in Ref. [8], one can use a scaling ansatz for the probability of events in the spreading process $p(x, \delta t)$ (x is the distance of the event from the original site, δt the elapsed time) which in particular allows to consider the nearest neighbors of an active site (i.e., of a beam that breaks). In our case this is complicated by the fact that, due to decreasing front velocity, the breaking rate of beams goes down, but on the other hand, the response time of the front stays the same. Thus we use the scaling

$$p(1, \delta t) \propto \delta t^{-1/z}. \quad (6)$$

This is valid for intermediate times such that the breaking events are still correlated, and not dependent on the breaking rate. The large- t contribution indicates a mean-field background, that has first to be subtracted from $p(1, \delta t)$ to obtain the real scaling behavior. Although it is hard to determine the exact upper limit of the regime in which scaling can be expected, the result is nevertheless consistent with $z=4/3$ as is evident from Fig. 5.

As a general conclusion, it is quite obvious that our elastic lattice model leads to a crack front geometry which is consistent with that of Eq. (1). The perturbative results are thus in agreement with our simulation results for a thin, three-dimensional system. This makes the discrepancy in ζ between theory and the experiment of Ref. [2] even more difficult to understand. There is however a variety of possible explanations, and several of them are discussed in Refs. [3,4]. An example of such an explanation would be the effect of acoustic emission from a local fracture that may be quali-

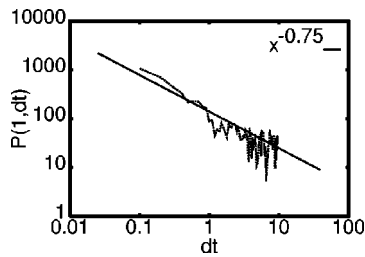


FIG. 5. The simulation results for Eq. (6) compared with the perturbative solution $z=4/3$.

tatively different in the experiments and in our numerical model. In the simulations, acoustic emission have at most a minor effect. Another possibility is that the disorder in the experiment may differ qualitatively from the uncorrelated disorder assumed in most models and used in our simulations. Both power-law amplitude distributions (of, e.g., the local breaking stress) and correlated patches would lead at the very least to a crossover lengthscale, below which the asymptotic scaling would be modified [15]. This crossover scale could obscure comparisons between the model results and the experiments.

A closer look at the relations between different length scales in the experiment [2] reveals, however, that a result that would exactly correspond to our model result is actually impossible. The geometry of the crack front in our numerical model is a result of competition between the uncorrelated disorder and the stress concentration effects. The former increases roughness, while the latter tends to decrease it. The stress concentration is governed by the bending of the elastic plates in the direction perpendicular to the crack propagation.

In the experiment the disorder was introduced by a sand-blasting procedure with a bead size of $50 \mu\text{m}$, while the elastic plate in the experiment were 4 mm thick. Bending of an elastic plate is in practice possible only overlength scales which are considerably larger than the thickness of the plate. By comparing the length scales of the disorder and the plate thickness (i.e., μm and mm), it is easy to see that in the experiment roughness cannot arise from the same competing mechanism as in the numerical model. Furthermore, in the experiment the roughness of the fronts was established on length scales up to a few millimeters, while the fronts appeared more or less flat on larger length scales. This proves again that bending of the plates cannot be responsible for the roughness of the crack front as it should then appear *only* on length scales larger than the mm scale. With a bead size of $50 \mu\text{m}$ one would expect that the variance of the local strength on the mm scale should be very small, which is consistent with a flat front on the larger length scales. In the numerical model we found that the front roughness vanishes rapidly with decreasing disorder as is only to be expected.

In summary, we have investigated a lattice model for the roughening of a propagating planar crack, which is confined between two coupled elastic plates. The front roughness appears as a result of heterogeneous material strength, i.e., disorder. Due to the long-range nature of the front elasticity, it is worth noting that the inclusion of bulk damage does not change our conclusions. The kinetic roughening is found to belong to the same universality class with the corresponding continuum models. Based on our model, we would expect that in experiments where the scale of the disorder is comparable with the thickness of the plate, i.e., for, e.g., thin elastic plates, a scaling more in line with model predictions would be found.

-
- [1] B.B. Mandelbrot, D.E. Passoja, and A.J. Paullay, *Nature (London)* **308**, 721 (1984).
- [2] A. Delaplace, J. Schmittbuhl, and K.J. Måløy, *Phys. Rev. E* **60**, 1337 (1999).
- [3] E. Bouchaud, *J. Phys.: Condens. Matter* **9**, 4319 (1997).
- [4] E. Bouchaud and F. Paun, *Comput. Sci. Eng.* **1**, 32 (1999).
- [5] H. Gao and J.R. Rice, *J. Appl. Mech.* **56**, 828 (1989).
- [6] J. Schmittbuhl, S. Roux, J.P. Vilotte, and K.J. Måløy, *Phys. Rev. Lett.* **74**, 1787 (1995).
- [7] S. Ramanathan and D. Fisher, *Phys. Rev. Lett.* **79**, 877 (1997).
- [8] A. Tanguy, M. Gounelle, and S. Roux, *Phys. Rev. E* **58**, 1577 (1999).
- [9] D. Ertaş and M. Kardar, *Phys. Rev. E* **49**, R2532 (1994).
- [10] The method is similar to that used in the time-dependent finite element method.
- [11] J. Åström, M. Kellomäki, M. Alava, and J. Timonen, *Phys. Rev. E* **56**, 6042 (1997).
- [12] See e.g., L. D. Landau and E. M. Lifshitz, *Theory of Elasticity*, (Pergamon, New York, 1958).
- [13] S. Zapperi, H.J. Herrmann, and S. Roux, e-print cond-mat/0003468.
- [14] A similar problem due to the lack of time-translational invariance has been discussed in M. Dubé *et al.*, *Phys. Rev. Lett.* **83**, 1628 (1999).
- [15] M. Myllys *et al.*, *Phys. Rev. Lett.* **84**, 1946 (2000).